

LOAN COPY: RETURN TO  
AFWL TECHNICAL LIBRARY  
KIRTLAND AFB, N.M.

NASA  
TP  
1646  
c.1

# NASA Technical Paper 1646

## Damping in Tapered Annular Seals for an Incompressible Fluid

David P. Fleming

APRIL 1980

1646-7



TECH LIBRARY KAFB, NM

NASA



0134591

## NASA Technical Paper 1646

# Damping in Tapered Annular Seals for an Incompressible Fluid

David P. Fleming  
*Lewis Research Center*  
*Cleveland, Ohio*

**NASA**  
National Aeronautics  
and Space Administration

**Scientific and Technical  
Information Office**

1980

## SUMMARY

An analysis is presented to calculate damping in annular seals for an incompressible fluid. Results show that damping in tapered seals (optimized for stiffness) is considerably less than that in straight seals for the same minimum clearance. Damping in rotating seals can promote fractional frequency whirl.

Results were obtained with and without the fluid temporal acceleration term  $\partial u / \partial t$ . Neglecting fluid acceleration led to errors in calculated damping of up to 16 percent. However, this is considered acceptable for a large class of practical application.

## INTRODUCTION

It is now well recognized that annular pressure seals can have a considerable influence on the dynamic behavior of rotors. This is not surprising when one considers that such a seal has the appearance of a journal bearing, although with larger clearances than is usual in bearing practice. Most of the force generated in a seal is due to the high velocity throughflow of sealed fluid. In a series of papers (refs. 1 to 3) Black and his coworkers calculated stiffness and damping in annular seals having constant clearance in the axial direction and sealing an incompressible fluid. Allaire, et al. (ref. 4) extended the analysis to seals with large eccentricities; however, they neglected the effect of fluid temporal acceleration without fully understanding the errors produced. In reference 5, Fleming showed that stiffness could be considerably increased by configuring the seal so that the clearance is greater at the inlet than at the exit. The higher stiffness can be beneficial in stabilizing rotors by shifting critical speeds; floating-ring seals can also benefit from higher stiffness with resulting longer life.

It is recognized that damping, as well as stiffness, influences seal behavior. Thus the purpose of this report is to calculate damping for the tapered seal configurations which were analyzed for stiffness in reference 5. A second purpose is to fully determine the errors produced by neglecting fluid acceleration. If reasonable accuracy can be obtained with the simpler procedure, analyses of more complex situations (e.g., compressible fluids) will be greatly eased.

## SYMBOLS

A	integration constant
B	damping, N-sec/m
$\bar{B}$	dimensionless damping, $BC_2/L^2D\sqrt{p_0\rho}$
C	seal radial clearance (concentric), m
D	seal diameter, m
E	inertia coefficient, kg
$\bar{E}$	dimensionless inertia, $EC_2/\rho DL^3$
e	seal displacement, m
F	seal force, N
f	integral (eq. (26))
G	$H - 1$
H	clearance ratio, $C_1/C_2$
h	local film thickness, m
J	defined by eq. (18)
K	stiffness, N/m
$\bar{K}$	dimensionless stiffness, $KC_2/p_0 LD$
L	seal length, m
M	seal leakage flow, kg/sec
$\bar{M}$	dimensionless leakage, $M/\pi DC_2 \sqrt{p_0\rho}$
p	pressure, N/m <sup>2</sup>
R	seal radius, m
S	defined by eq. (19)
t	time, sec
u	fluid velocity, m/sec
V	$\partial h/\partial t$
x, y	coordinates normal to seal axis

$z$	axial coordinate
$\alpha$	taper angle
$\Delta$	$\partial/\partial t$
$\epsilon$	eccentricity ratio, $e/C_2$
$\eta$	total entrance loss factor, $1 + \xi$
$\theta$	angular coordinate
$\lambda$	friction factor
$\xi$	entrance loss factor
$\rho$	fluid density, $\text{kg}/\text{m}^3$
$\sigma$	$\lambda L/C_2$
$\omega$	angular speed, rad/sec

Subscripts:

$p$	precessional
$r$	radial direction or rotational
$s$	steady concentric condition
$t$	perturbed condition or tangential direction
$0$	upstream stagnation condition or zero order in time
$1$	seal entrance or first order in time
$2$	seal exit or second order in time

## ANALYSIS

The configuration to be analyzed is that of an annular clearance seal whose clearance decreases in the flow direction (fig. 1). Around the circumference, the clearance is given by

$$h(z, \theta, t) = C(z) + C_2 \epsilon(t) \cos \theta$$

where  $C$  is the clearance for a concentric seal. This implies that the only motion considered is in the plane  $\theta = 0$ .

$$C(z) = C_1 - \alpha z$$

The notation  $C_1 = C(0)$  and  $C_2 = C(L)$  is used. When the seal is eccentric ( $\epsilon \neq 0$ ) or has a velocity or acceleration in the radial direction, a radial force is generated. To determine this force, the pressure distribution within the seal will be calculated and integrated over the seal area. In common with references 1 to 5, the following assumptions are employed:

(1) The fluid is incompressible.

(2) Rotational effects on the flow field are neglected; the flow is one-dimensional in the axial direction.

In addition, as in references 1, 2, and 5:

(3) Eccentricity is small compared with the concentric clearance, that is,  $\epsilon \ll 1$ .

(4) Friction factor is constant everywhere within the seal. Reference 3 shows that this introduces some error for the Reynolds number range where the friction factor is Reynolds number dependent. In the case of a high Reynolds number, however, friction factor no longer varies with Reynolds number (ref. 6).

### Development of Equations

As in reference 5, we start with the continuity and momentum equations. These expressions differ from those of references 1 and 4 because the clearance  $h$  varies along the length in a tapered seal.

$$h \frac{\partial u}{\partial z} + u \frac{\partial h}{\partial z} + \frac{\partial h}{\partial t} = 0 \quad (1)$$

$$-\frac{1}{\rho} \frac{\partial p}{\partial z} = \lambda \frac{u^2}{h} + u \frac{\partial u}{\partial z} + \frac{\partial u}{\partial t} \quad (2)$$

The boundary conditions are as follows:

$$\left. \begin{aligned} p = p_0 &= \eta \frac{\rho u^2}{2} & \text{at } z = 0 \\ p &= 0 & \text{at } z = L \end{aligned} \right\} \quad (3)$$

Variables  $h$ ,  $u$ , and  $p$  will now be expressed as the sum of a steady state concentric value and a perturbation which will be assumed small compared to the steady-state value. Thus,

$$\left. \begin{array}{l} h = C + h_t \\ u = u_s + u_t \\ p = p_s + p_t \end{array} \right\} \quad (4)$$

The continuity and momentum equations may then be divided into separate expressions involving steady-state and perturbed variables. The steady-state expressions are

$$C \frac{du_s}{dz} + u_s \frac{dC}{dz} = 0 \quad (5)$$

$$-\frac{1}{\rho} \frac{dp_s}{dz} = \lambda \frac{u_s^2}{C} + u_s \frac{du_s}{dz} \quad (6)$$

with the following boundary conditions:

$$\left. \begin{array}{l} p_s = p_0 - \frac{\eta \rho u_s^2}{2} \quad \text{at } z = 0 \\ p_s = 0 \quad \text{at } z = L \end{array} \right\} \quad (7)$$

where  $\eta = 1 + \xi$  is the total entrance loss factor. The perturbed variable expressions (in which products of two perturbed variables are neglected) are

$$h_t \frac{du_s}{dz} + C \frac{\partial u_t}{\partial z} + u_t \frac{dC}{dz} + \frac{\partial h_t}{\partial t} = 0 \quad (8)$$

$$-\frac{1}{\rho} \frac{\partial p_t}{\partial z} = 2\lambda \frac{u_s u_t}{C} - \lambda \frac{u_s^2 h_t}{C^2} + u_s \frac{\partial u_t}{\partial z} + u_t \frac{du_s}{dz} + \frac{\partial u_t}{\partial t} \quad (9)$$

The boundary conditions are

$$\left. \begin{array}{l} p_t = -\eta \rho u_s u_t \quad \text{at } z = 0 \\ p_t = 0 \quad \text{at } z = L \end{array} \right\} \quad (10)$$

Steady state equations (5) and (6) are easily solved:

$$u_s = \frac{u_1 C_1}{C} \quad (11)$$

$$p_s = \frac{1}{2} \rho u_1^2 C_1^2 \left( \frac{\lambda}{\alpha} + 1 \right) \left( \frac{1}{C_2^2} - \frac{1}{C^2} \right) \quad (12)$$

$$u_1^2 = \frac{2p_0}{\rho \left[ \eta + \left( \frac{\lambda}{\alpha} + 1 \right) (H^2 - 1) \right]} \quad (13)$$

The solution of equation (8) is

$$u_t = \frac{A}{C} - \frac{h_t u_1 C_1}{C^2} + \frac{V}{\alpha} \quad (14)$$

where  $A$  is an integration function and

$$V \equiv \frac{\partial h_t}{\partial t} \quad (15)$$

There are alternative methods for solving the perturbed momentum equation (9). One method is to retain all the terms and solve the equation as Black did in reference 1. Another method is to neglect the fluid temporal acceleration term,  $\partial u_t / \partial t$ , as Allaire, et al., did in reference 4. This would introduce greater approximation but the accuracy may be acceptable given the much easier solution procedure. Both methods will be presented in order that a comparison of the results may be made.

#### Solution Retaining Fluid Temporal Acceleration $\partial u / \partial t$

Equations (11) and (14) are substituted in equation (9) to obtain

$$-\frac{1}{\rho} \frac{\partial p_t}{\partial z} = -\frac{3h_t u_1^2 C_1^2}{C^4} (\lambda + \alpha) + \frac{2u_1 C_1 A}{C^3} (\lambda + \alpha) + \frac{2\lambda u_1 C_1 V}{\alpha C^2} + \frac{\dot{A}}{C} + \frac{\dot{V}}{\alpha} \quad (16)$$

where the dot denotes differentiation with respect to time; that is,  $\dot{A} = \partial A / \partial t$  and  $\dot{V} = \partial V / \partial t = \partial^2 h_t / \partial t^2$ . This expression may be immediately integrated and the boundary condition  $p_t = 0$  at  $z = L$  applied to obtain

$$\begin{aligned}
-\frac{p_t}{\rho} = & -h_t u_1^2 C_1^2 \left(1 + \frac{\lambda}{\alpha}\right) \left(\frac{1}{C^3} - \frac{1}{C_2^3}\right) + u_1 C_1 A \left(1 + \frac{\lambda}{\alpha}\right) \left(\frac{1}{C^2} - \frac{1}{C_2^2}\right) \\
& + \frac{2\lambda u_1 C_1 V}{\alpha^2} \left(\frac{1}{C} - \frac{1}{C_2}\right) - \frac{\dot{A}}{\alpha} \ln \frac{C}{C_2} + \frac{\dot{V}}{\alpha} (z - L) \quad (17)
\end{aligned}$$

The boundary condition at  $z = 0$ , equation (10), may be applied to find the integration function  $A$ . As a first step, all terms containing  $A$  are moved to the left side of the equation; thus,

$$\begin{aligned}
u_1 A \left[ \eta + (\sigma + G)(H + 1) \right] + \frac{\dot{A}HL}{G} \ln H = & u_1^2 h_t \left[ \eta + (\sigma + G)(H^2 + H + 1) \right] \\
& - \frac{u_1 VHL}{G} (\eta + 2\sigma) - \frac{\dot{VHL}^2}{G}
\end{aligned}$$

where  $H$  is the film thickness ratio  $C_1/C_2$ ,  $G \equiv H - 1$ ,  $\sigma = \lambda L/C_2$ , and  $\alpha$  has been replaced by its equivalent in terms of film thickness ratio:  $\alpha = GC_2/L$ .

This equation cannot be solved in the conventional manner because both  $A$  and its time derivative appear. However, the equation may be rewritten using differential operators (ref. 7).

$$\left( u_1 J + \frac{HL \ln H}{G} \Delta \right) A = \left[ u_1^2 S - \frac{u_1 HL}{G} (\eta + 2\sigma) \Delta - \frac{HL^2}{G} \Delta^2 \right] h_t$$

where  $\Delta \equiv \partial/\partial t$  and, to simplify the writing, the substitutions

$$J \equiv \eta + (\sigma + G)(H + 1) \quad (18)$$

and

$$S \equiv \eta + (\sigma + G)(H^2 + H + 1) \quad (19)$$

have been made. This has the appearance of an algebraic equation and, indeed, it is common practice to treat  $\Delta$  as an algebraic quantity. The following procedure to determine  $A$  was used by Black in reference 1. A straightforward algebraic solution for  $A$  yields

$$A = \frac{u_1^2 S - \left[ \frac{u_1 H L (\eta + 2\sigma)}{G} \right] \Delta - \frac{H L^2}{G} \Delta^2}{u_1 J + \frac{H L \ln H}{G} \Delta} h_t \quad (20)$$

For high axial flow rates, the first term of the denominator is much larger than the second; hence a binomial expansion of three terms will be a good approximation. Truncating at three terms is equivalent to neglecting the effect of time derivatives higher than the second on the seal pressures. With this substitution, equation (20) becomes

$$A = \frac{1}{u_1 J} \left[ u_1^2 S - \frac{u_1 H L}{G} (\eta + 2\sigma) \Delta - \frac{H L^2}{G} \Delta^2 \right] \left( 1 - \frac{H L \ln H}{u_1 J G} \Delta + \frac{H^2 L^2 \ln^2 H}{u_1^2 J^2 G^2} \Delta^2 \right) h_t \quad (21)$$

This is next multiplied out, and coefficients of various powers of  $\Delta$  collected, ignoring coefficients of  $\Delta^3$  and higher powers. Making the definition

$$A = (A_0 + A_1 \Delta + A_2 \Delta^2) h_t \quad (22)$$

we obtain

$$A_0 = \frac{u_1 S}{J} \quad (23)$$

$$A_1 = - \frac{H L}{G J} \left( \frac{S \ln H}{J} + \eta + 2\sigma \right) \quad (24)$$

$$A_2 = \frac{H L^2}{u_1 J G} \left[ \frac{S H \ln^2 H}{J^2 G} + \frac{H \ln H}{J G} (\eta + 2\sigma) - 1 \right] \quad (25)$$

With the axial pressure profile known, equation (17) may now be integrated to determine the force on an axial strip. (It is not necessary to consider the contribution of  $p_s$ , as it is uniform around the circumference and the net force from it is zero.) After some algebraic manipulation,

$$f \equiv \int_0^L -\frac{p_t}{\rho} dz = \frac{h_t u_1^2 L (1 + 2H)(\sigma + G)}{2C_2} + \frac{2\sigma u_1 V L^2 H \left( \frac{\ln H}{G} - 1 \right)}{C_2 G^2} - \frac{\dot{A} L^2}{G C_2} \left( \frac{H \ln H}{G} - 1 \right) - \frac{\dot{V} L^3}{2G C_2} - \frac{A u_1 L (\sigma + G)}{C_2} \quad (26)$$

Similar to equation (22), define

$$f = (f_0 + f_1 \Delta + f_2 \Delta^2) h_t \quad (27)$$

Then, substituting equations (22) to (25) in equation (26) results in

$$f_0 = \frac{u_1^2 L}{C_2} (\sigma + G) \left( H + \frac{1}{2} - \frac{S}{J} \right) \quad (28)$$

$$f_1 = \frac{u_1 L^2}{G C_2} \left[ \frac{2\sigma H}{G} \left( \frac{\ln H}{G} - 1 \right) + \frac{H}{J} (\sigma + G) \left( \frac{S \ln H}{J} + \eta + 2\sigma \right) - \frac{S}{J} \left( \frac{H \ln H}{G} - 1 \right) \right] \quad (29)$$

$$f_2 = \frac{L^3}{C_2 G} \left\{ \frac{H}{GJ} \left( \frac{S \ln H}{J} + \eta + 2\sigma \right) \left( \frac{H \ln H}{G} - 1 \right) - \frac{1}{2} - \frac{H(\sigma + G)}{J} \left[ \frac{SH \ln^2 H}{GJ^2} + \frac{H \ln H}{GJ} (\eta + 2\sigma) - 1 \right] \right\} \quad (30)$$

The total seal force is now found by integrating around the seal circumference

$$F = \int_0^{2\pi} \rho f \cos \theta \ R \ d\theta \quad (31)$$

The perturbed clearance  $h_t$  varies around the circumference according to

$$h_t = h_{t0} \cos \theta \quad (32)$$

where  $h_{t0}$  is the amplitude of the perturbation at  $\theta = 0$ . Thus

$$F = \int_0^{2\pi} \rho (f_0 + f_1 \Delta + f_2 \Delta^2) h_{t0} \cos^2 \theta R d\theta$$

$$F = \pi \rho R (f_0 + f_1 \Delta + f_2 \Delta^2) h_{t0} \quad (33)$$

In terms of stiffness, damping, and inertia coefficients,

$$F = (K + B \Delta + E \Delta^2) h_t \quad (34)$$

It is convenient to present results in terms of the following dimensionless coefficients:

Stiffness

$$\bar{K} = \frac{KC_2}{p_0 LD} = \frac{\pi}{J} (\sigma + G) \left( \frac{1}{2} + H - \frac{S}{J} \right) \quad (35)$$

Damping

$$\bar{B} = \frac{BC_2}{L^2 D \sqrt{p_0 \rho}} = \frac{\pi}{G \sqrt{2J}} \left[ \frac{2\sigma H}{G} \left( \frac{\ln H}{G} - 1 \right) + \frac{H}{J} (\sigma + G) \left( \frac{S \ln H}{J} + \eta + 2\sigma \right) - \frac{S}{J} \left( \frac{H \ln H}{G} - 1 \right) \right] \quad (36)$$

Inertia

$$\begin{aligned} \bar{E} = \frac{EC_2}{\rho DL^3} &= \frac{\pi}{2G} \left\{ \frac{H}{GJ} \left( \frac{S \ln H}{J} + \eta + 2\sigma \right) \left( \frac{H \ln H}{G} - 1 \right) \right. \\ &\quad \left. - \frac{1}{2} - \frac{H(\sigma + G)}{J} \left[ \frac{SH \ln^2 H}{GJ^2} + \frac{H \ln H}{GJ} (\eta + 2\sigma) - 1 \right] \right\} \quad (37) \end{aligned}$$

It may be verified that these results reduce to those presented by Black and Jensen (ref. 2) as  $H$  tends to 1.

Solution Neglecting Fluid Temporal Acceleration  $\partial u / \partial t$

When the fluid temporal acceleration is neglected, the momentum equation (9) becomes

$$-\frac{1}{\rho} \frac{\partial p_t}{\partial z} = 2\lambda \frac{u_s u_t}{C} - \lambda \frac{u_s^2 h_t}{C^2} + u_s \frac{\partial u_t}{\partial z} + u_t \frac{du_s}{dz} \quad (38)$$

Equations (11) and (14) for  $u_s$  and  $u_t$ , respectively, are substituted in this, the result integrated in  $z$ , and the boundary condition at  $z = L$  applied to obtain

$$\begin{aligned} -\frac{p_t}{\rho} = & -h_t u_1^2 C^2 \left(1 + \frac{\lambda}{\alpha}\right) \left(\frac{1}{C^3} - \frac{1}{C_2^3}\right) + u_1 C_1 A \left(1 + \frac{\lambda}{\alpha}\right) \left(\frac{1}{C^2} - \frac{1}{C_2^2}\right) \\ & + \frac{V u_1 C_1}{\alpha} \left(\frac{2\lambda}{\alpha} + 1\right) \left(\frac{1}{C} - \frac{1}{C_2}\right) \end{aligned} \quad (39)$$

The integration function  $A$  is readily found by applying the boundary condition (eq. (7)) at  $z = 0$  resulting in

$$A = \frac{1}{J} \left[ h_t u_1 S - \frac{V H L (\eta + 2\sigma + G)}{G} \right] \quad (40)$$

Substitution of this into equation (39) and integration to determine seal forces is straightforward. The result for seal stiffness is identical to that for the more complete solution, as expected. For damping,

$$\bar{B} = \frac{\pi H}{G \sqrt{2J}} \left[ \frac{(\eta + 2\sigma + G)(\sigma + G)}{J} + \left(\frac{2\sigma}{G} + 1\right) \left(\frac{\ln H}{G} - 1\right) \right] \quad (41)$$

The inertia term does not appear.

## RESULTS

The preceding analysis has been used to calculate values of seal damping and inertia terms for tapered seals. Straight seal (zero taper angle) results are also presented for comparison; they were calculated from the expressions in references 1 and 2. It also may be verified that the expressions for tapered seal results presented herein reduce to those for straight seals in reference 2 as the clearance ratio  $H$  tends toward 1. Tapered and straight seals are compared using the same minimum clearance, since this is the significant dimension in practical seal design.

Values of dimensionless damping coefficient  $\bar{B}$  appear in figure 2 for a range of dimensionless seal length  $\sigma$  and with entrance loss factor  $\xi = 0$ . (For turbulent flow  $\xi$  is at most 0.2; results are not much different than for  $\xi = 0$ . This was also shown by Black (ref. 2) for straight seals.) Results are shown for both straight seals and for seals whose taper is optimized to maximize the stiffness to leakage ratio (ref. 5). For each seal, results are shown for the full solution (retaining  $\partial u / \partial t$ ) and for the approximate solution (neglecting  $\partial u / \partial t$ ).

Damping values are always higher for a straight seal, as would be expected since the average clearance is lower. The difference is least near a length  $\sigma$  of about 1.5, where the straight seal damping is minimum. Tapered seal damping is nearly constant out to  $\sigma \sim 3$ ; damping then increases with  $\sigma$ . The approximate solution errs in opposite directions for straight and tapered seals. For straight seals, the solution neglecting  $\partial u / \partial t$  overestimates damping up to 16 percent. For the optimum tapered seals, the approximate solution underestimates damping a maximum of 10 percent. These errors are considerably greater than those implied by the authors of reference 4, but are still considered quite acceptable by the author.

The inertia term  $\bar{E}$  is shown in figure 3 for the full solution. (The approximate solution does not yield the inertia term at all.) For the optimum tapered seal  $\bar{E}$  is very nearly constant over the entire range of seal length shown. For the straight seal  $\bar{E}$  is negative for very small seal length; it increases rapidly with length and for large lengths becomes nearly constant at a value somewhat greater than for a tapered seal. Negative results are not shown in reference 2, but this appears to be due simply to insufficient points having been plotted for small seal length.

#### Effect of Seal Rotation

The calculations so far have neglected any seal rotation. For a rotating seal, according to the coordinate transformation used by Black and Jenssen (ref. 2), the forces on the seal journal are given by

$$\begin{bmatrix} F_x \\ F_y \end{bmatrix} = - \begin{bmatrix} K - \frac{1}{4} E \omega_r^2 & \frac{1}{2} B \omega_r \\ -\frac{1}{2} B \omega_r & K - \frac{1}{4} E \omega_r^2 \end{bmatrix} \begin{bmatrix} x \\ y \end{bmatrix} - \begin{bmatrix} B & E \omega_r \\ -E \omega_r & B \end{bmatrix} \begin{bmatrix} \dot{x} \\ \dot{y} \end{bmatrix} - \begin{bmatrix} E & 0 \\ 0 & E \end{bmatrix} \begin{bmatrix} \ddot{x} \\ \ddot{y} \end{bmatrix} \quad (42)$$

In equation (42),  $\omega_r$  is the shaft rotational speed. Recall that rotational effects were neglected in determining the seal coefficients  $K$ ,  $B$ , and  $E$ . Thus one would expect equation (42) to be valid only for small rotational speeds; that is,  $R\omega_r \ll u_1$ .

The seal journal is now considered to be precessing in a circular orbit about the seal center with orbital frequency  $\omega_p$ . For this condition we will calculate the radial restoring force and the tangential (whirl direction) force. Since the seal has circular symmetry, it is sufficient to examine the situation when the seal journal center lies along the  $x$ -axis, that is, when  $x = e$  and  $y = 0$ . Then  $\dot{x} = 0$ ,  $\dot{y} = e\omega_p$ ,  $\ddot{x} = -e\omega_p^2$ ,  $\ddot{y} = 0$ . The radial and tangential forces are

$$\left. \begin{aligned} F_r &= -\left(K - \frac{1}{4}E\omega_r^2\right)e - Ee\omega_r\omega_p + Ee\omega_p^2 \\ F_t &= \frac{1}{2}Be\omega_r - Be\omega_p \end{aligned} \right\} \quad (43)$$

These expressions may be rewritten as

$$\left. \begin{aligned} -K_r &= \frac{F_r}{e} = -K + E\omega_r^2 \left( \frac{1}{4} - \frac{\omega_p}{\omega_r} + \frac{\omega_p^2}{\omega_r^2} \right) \\ -K_t &= \frac{F_t}{e} = B\omega_r \left( \frac{1}{2} - \frac{\omega_p}{\omega_r} \right) \end{aligned} \right\} \quad (44)$$

Note that  $e$  is by definition in the radial direction. Two conclusions may be drawn from these expressions:

(1) The inertia term is a perturbation on the seal radial restoring force. If only whirl ratios  $\omega_p/\omega_r$  from 0 to 1 are considered, this perturbation has a maximum value at 0 and 1 and becomes zero for  $\omega_p/\omega_r = 1/2$ .

(2) The tangential force promotes forward whirl when  $\omega_p/\omega_r < 1/2$ , inhibits whirl when  $\omega_p/\omega_r > 1/2$ , and is zero for half-frequency whirl ( $\omega_p/\omega_r = 1/2$ ). This is remarkably similar to the situation in a full circular journal bearing. The seal differs from a journal bearing in the radial force being a maximum for  $\omega_p/\omega_r = 1/2$  (assuming  $E > 0$ , which is always the case for a tapered seal and is true for all but small seal lengths for a straight seal). We may also infer that damping in a rotating seal is not entirely beneficial. The damping term produces a tangential force which inhibits synchronous whirl but promotes whirl at half-frequency or less.

### Numerical Example

Seal damping and inertia have been presented in dimensionless form, as were stiffness and leakage flow in reference 5. Tapered and straight seal stiffness and leakage flow from reference 5, as well as optimum clearance ratios, appear in figures 4 to 6. Also, damping and inertia forces vary with rotor speed. Thus the relative size of the various terms can only be compared for specific examples. The example chosen here is the space shuttle main engine (SSME) high pressure fuel turbopump (HPFTP) inter-stage seals that were examined in reference 5. These seals are 76 millimeters in diameter, 43 millimeters long, and have a radial clearance of 0.13 millimeters. The fluid sealed is liquid hydrogen; the pressure difference across the seal is 140 bars at the rotor design speed of 37 000 rpm (ref. 4). As determined in reference 5, the dimensionless seal length  $\sigma$  is 2.4. Seal coefficients are presented in table I for straight seals and for optimum tapered seals. Tapered seal stiffness is more than twice that of the straight seal. The tapered seal damping and inertia terms are 20 to 25 percent less than the corresponding straight seal quantities. Also shown in table I are the terms  $B\omega_r$  and  $E\omega_r^2$  which appear in equation (44). These terms have the dimensions of stiffness and may be compared with the stiffness term. For the straight seal, damping in the form  $B\omega_r$  is much greater than the stiffness term, while for the tapered seal  $B\omega_r$  is somewhat less than  $K$ . The inertia term  $E\omega_r^2$  is quite small for both straight and tapered seals.

The coefficients from table I may be used with equation (44) to yield radial and tangential forces per unit radial displacement for various whirl ratios (ratios of precessional to rotational speed). These are shown in table II for whirl ratios of 0 (no precession), 1/2, and 1 (synchronous precession). For the case of no precession, radial forces are reduced slightly from the stiffness of table I due to the inertia term. The damping term transforms to a negative tangential force, which means that there is a whirl-promoting force on the seal journal. This tangential force is analogous to the tangential force in a journal bearing. For the straight seal, the tangential force is somewhat larger than the radial force, while for the tapered seal, tangential force is only one-third of the radial force. For a whirl ratio of one-half, the inertia effect disappears, and the radial force is equal to the nonrotating force of table I, while the tangential force is zero. For synchronous precession ( $\omega_p/\omega_r = 1$ ), radial forces are identical to the zero-precession case, and tangential forces are identical in magnitude but of opposite sign to the zero-precession case. The tangential force is thus a strong inhibitor of synchronous precession.

## SUMMARY OF RESULTS

An analysis was performed to calculate the damping in tapered annular seals for an incompressible fluid. Results show that damping in optimized tapered seals is considerably less than that in straight seals for the same minimum clearance. It was also pointed out that damping in rotating seals is not entirely beneficial, as it can sometimes promote whirl.

Results were obtained with and without the inclusion of the fluid temporal acceleration term  $\partial u / \partial t$ . Neglecting fluid acceleration led to errors in calculated damping of up to 16 percent. However, this is considered acceptable because of the much greater ease of obtaining a solution.

Lewis Research Center,  
National Aeronautics and Space Administration,  
Cleveland, Ohio, November 16, 1979,  
505-04.

## REFERENCES

1. Black, H. F.: Effects of Hydraulic Forces in Annular Pressure Seals on the Vibrations of Centrifugal Pump Rotors. *J. Mech. Eng. Sci.*, vol. 11, no. 2, Apr. 1969, pp. 206-213.
2. Black, H. F.; and Jenssen, D. N.: Dynamic Hybrid Bearing Characteristics of Annular Controlled Leakage Seals. *Proc. Inst. Mech. Eng.*, vol. 184, pt. 3N, 1969-70, pp. 92-100.
3. Black, H. F.; and Jenssen, D. N.: Effects of High Pressure Ring Seals on Pump Rotor Vibrations. *ASME Paper 71-WA/FE-38*, Nov. 1971.
4. Allaire, P. E.; Lee, C. C.; and Gunter, E. J.: Dynamics of Short Eccentric Plain Seals with High Axial Reynolds Number. *J. Spacecr. Rockets*, vol. 15, no. 6, Nov.-Dec. 1978, pp. 341-347.
5. Fleming, D. P.: High Stiffness Seals for Rotor Critical Speed Control. *ASME Paper 77-DET-10*, Sep. 1977.
6. Knudsen, J. G.; and Katz, D. L.: *Fluid Dynamics and Heat Transfer*. McGraw Hill Book Co., Inc., 1958.
7. Rainville, Earl D.: *Elementary Differential Equations*. Macmillan Co., 1952.

TABLE I. - STIFFNESS, DAMPING, AND INERTIA  
 COEFFICIENTS FOR HPFTP STRAIGHT AND  
 TAPERED SEALS; ENTRANCE LOSS  $\xi = 0$

	Straight seal	Tapered seal
Dimensionless stiffness, $\bar{K}$	0.11	0.26
Stiffness, $K$ , MN/m	38	89
Dimensionless damping, $\bar{B}$	0.61	0.46
Damping, $B$ , (kN)(sec)/m	20	15
$B\omega_r$ , MN/m	79	59
Dimensionless inertia, $\bar{E}$	0.13	0.10
Inertia, $E$ , kg	.42	.33
$E\omega_r^2$ , MN/m	6	5

TABLE II. - RADIAL AND TANGENTIAL FORCES  
 PER UNIT RADIAL DISPLACEMENT FOR HPFTP  
 STRAIGHT AND TAPERED SEALS

[All forces in MN/m.]

Whirl ratio, $\omega_p/\omega_r$	Straight seal	Tapered seal
0	$K_r = 36$ $K_t = -39$	$K_r = 88$ $K_t = -30$
1/2	$K_r = 38$ $K_t = 0$	$K_r = 89$ $K_t = 0$
1	$K_r = 36$ $K_t = 39$	$K_r = 88$ $K_t = 30$

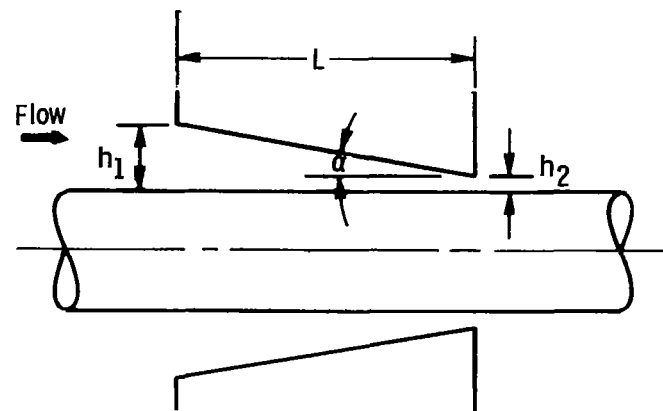


Figure 1. - Tapered annular seal.

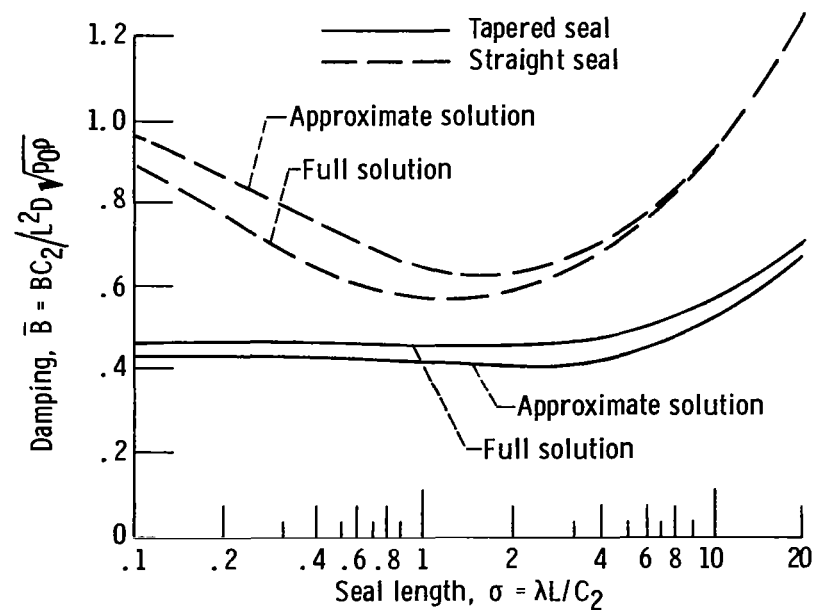


Figure 2. - Damping in tapered and straight seals. Entrance loss  $\xi = 0$ .

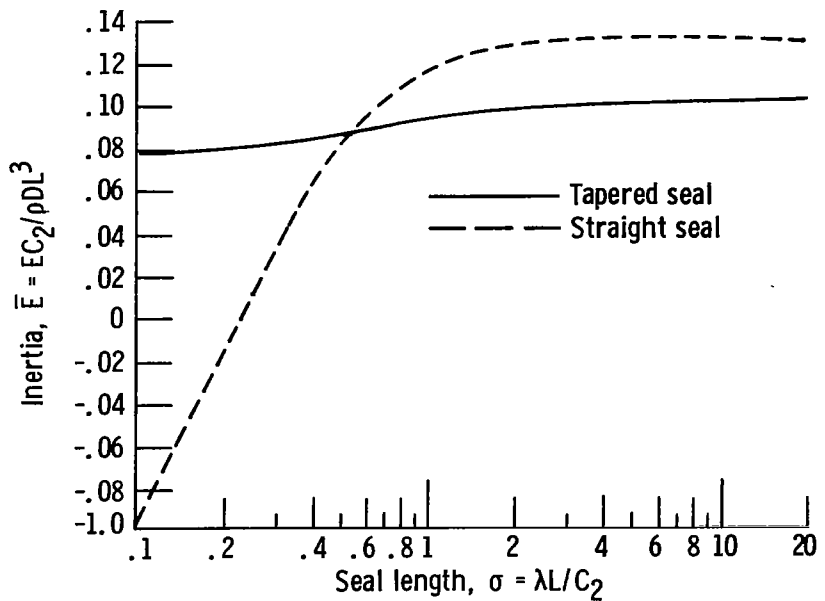


Figure 3. - Inertia term for tapered and straight seals.  
Entrance loss  $\xi = 0$ .

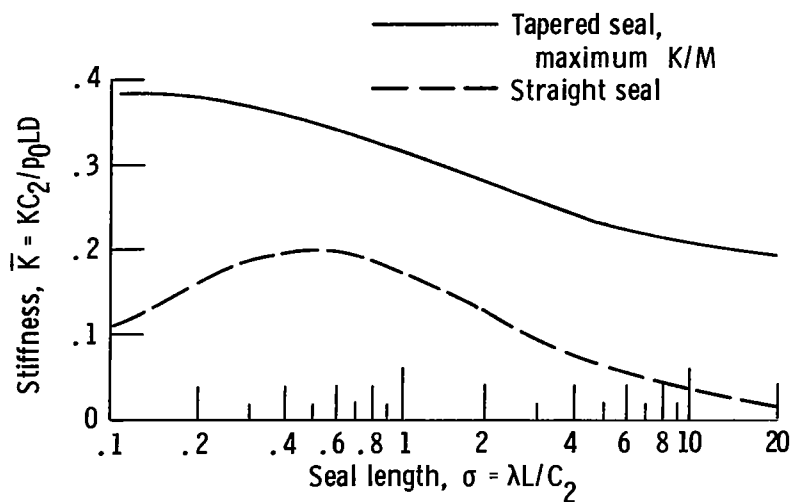


Figure 4. - Stiffness of tapered and straight seals. En-  
trance loss  $\xi = 0$ .

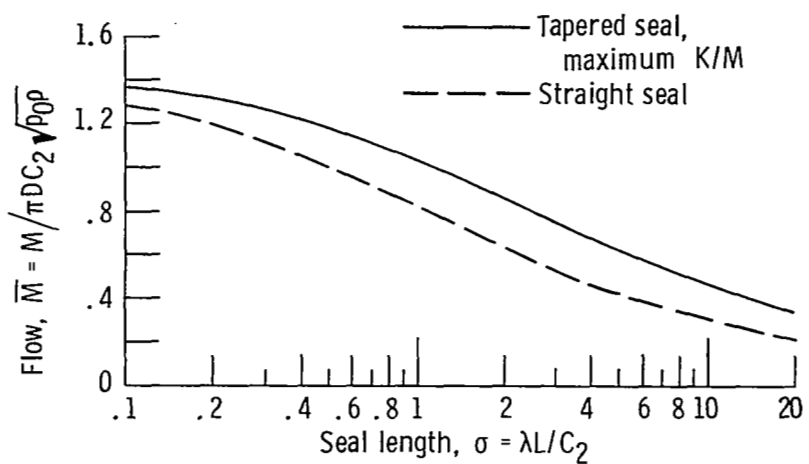


Figure 5. - Leakage flow through tapered and straight seals. Entrance loss  $\xi = 0$ .

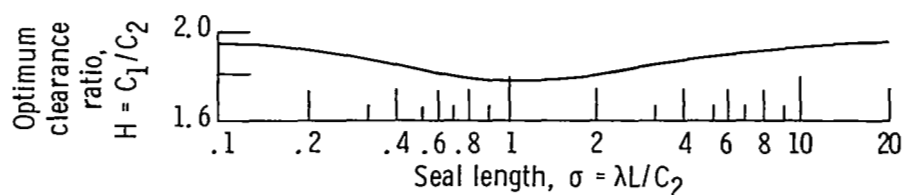


Figure 6. - Optimum clearance ratio for tapered seal. Entrance loss  $\xi = 0$ .

1. Report No. <b>NASA TP-1646</b>	2. Government Accession No.	3. Recipient's Catalog No.	
4. Title and Subtitle <b>DAMPING IN TAPERED ANNULAR SEALS FOR AN INCOMPRESSIBLE FLUID</b>		5. Report Date <b>April 1980</b>	
6. Performing Organization Code			
7. Author(s) <b>David P. Fleming</b>		8. Performing Organization Report No. <b>E-124</b>	
9. Performing Organization Name and Address <b>National Aeronautics and Space Administration Lewis Research Center Cleveland, Ohio 44135</b>		10. Work Unit No. <b>505-04</b>	
12. Sponsoring Agency Name and Address <b>National Aeronautics and Space Administration Washington, D.C. 20546</b>		11. Contract or Grant No.	
15. Supplementary Notes		13. Type of Report and Period Covered <b>Technical Paper</b>	
		14. Sponsoring Agency Code	
16. Abstract <p>An analysis is presented to calculate damping in annular seals for an incompressible fluid. Results show that damping in tapered seals (optimized for stiffness) is considerably less than that in straight seals for the same minimum clearance. Damping in rotating seals can promote fractional frequency whirl. Results were obtained with and without the fluid temporal acceleration term <math>\partial u / \partial t</math>. Neglecting fluid acceleration led to errors in calculated damping of up to 16 percent. However, this is considered acceptable for a large class of practical application.</p>			
17. Key Words (Suggested by Author(s)) <b>Annular seals Ring seals Seal damping</b>		18. Distribution Statement <b>Unclassified - unlimited STAR Category 37</b>	
19. Security Classif. (of this report) <b>Unclassified</b>	20. Security Classif. (of this page) <b>Unclassified</b>	21. No. of Pages <b>21</b>	22. Price* <b>A02</b>

\* For sale by the National Technical Information Service, Springfield, Virginia 22161

NASA-Langley, 1980

National Aeronautics and  
Space Administration

Washington, D.C.  
20546

Official Business

Penalty for Private Use, \$300

THIRD-CLASS BULK RATE

Postage and Fees Paid  
National Aeronautics and  
Space Administration  
NASA-451



3 1 1U,D, 021580 S00903DS  
DEPT OF THE AIR FORCE  
AF WEAPONS LABORATORY  
ATTN: TECHNICAL LIBRARY (SUL)  
KIRTLAND AFB NM 87117

POSTMASTER: If Undeliverable (Section 158  
Postal Manual) Do Not Return